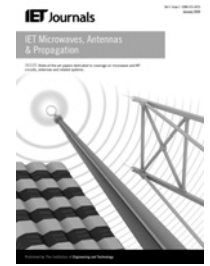


Published in IET Microwaves, Antennas & Propagation
 Received on 9th September 2013
 Revised on 16th June 2014
 Accepted on 10th July 2014
 doi: 10.1049/iet-map.2013.0498



ISSN 1751-8725

Field of a short dipole above a dielectric half-space with rough interface

Tsenchieh Chiu¹, Kamal Saraband²

¹Department of Electrical Engineering, National Central University, Zhongli City, Taoyuan County 32001, Taiwan

²Radiation Laboratory, Department of Electrical Engineering and Computer Science, The University of Michigan, Ann Arbor, MI 48109-2122, USA

E-mail: tcchiu@ee.ncu.edu.tw

Abstract: The accurate prediction of radiowave coverage at high frequency-ultra high frequency over irregular terrain features is of importance in the design and development of low-cost and low-power communication systems. This study studies the problem of electromagnetic wave propagation, excited by a short dipole, above a dielectric ground plane with an arbitrary dielectric profile and an irregular interface. This investigation is a natural extension of the classical Sommerfeld problem with the exception of the random surface irregularities at the interface between the two dielectric media. It is assumed that the interface profile height variations are small compared with the wavelength. First, the bistatic scattering of a plane wave illuminating the rough surface is solved using a perturbation solution of an integral equation for the induced polarisation current. Analytical expressions for the coherent field and incoherent scattered power at an arbitrary observation point are obtained. Then, the solutions for the coherent and incoherent scattered power generated by a small dipole of arbitrary orientation and position are derived by expanding the field of the dipole in terms of a continuous spectrum of plane waves and using superposition. The effects of the rough interface on the surface waves and on depolarisation are studied.

1 Introduction

With the rapid expansion of technology for mobile and wireless systems, an accurate method for prediction of radiowave propagation has become essential in the design and development of efficient, low-cost, low-power communication systems. In many communication scenarios where both the transmitter and receiver are near the ground, shadowing and multipath significantly affect the signal strength and the coherent bandwidth at the receiver. This is specifically the case for the propagation over irregular terrain. Terrain irregularity, so far as propagation is concerned, can be categorised into two groups: (i) large-scale roughness, and (ii) small-scale roughness. Large-scale terrain irregularities are generally referred to terrain irregularities large compared with the wavelength such as mountains and hills. Small-scale terrain irregularities, on the other hand, refer to surface roughnesses where the root-mean-square (rms) height and slope are small compared with the wavelength (at high frequency-ultra high frequency). These affect the wave propagation differently; for example, while large-scale terrain irregularities are the sources of shadowing and multipath, small-scale irregularities reduce the ground reflectivity and produce an incoherent field component because of surface scattering. Small-scale irregularities also affect the surface waves which are essential when both transmit and receive antennas are close to the air-ground interface.

Determination of the field of a small dipole over a half-space dielectric is a classical problem with a

well-known solution [1]. It is shown that when both the transmitter and receiver are near the surface, the contribution from surface waves is dominant. In practice, transmit and receive antennas of mobile units are usually very close (relative to the wavelength) to the ground. Existence of surface roughness may alter the contribution of surface waves drastically. In this case, the azimuthal symmetry of the problem may no longer be exploited, and the Sommerfeld solution must be modified significantly. The surface roughness generates an incoherent scattered field which is the source of depolarisation.

In this paper, the effect of slightly rough surfaces on the radiation of a short dipole is studied. In what follows, first, a solution for the scattered field (including the near field) from a slightly rough surface illuminated by plane waves is formulated in Sections 2 and 3. To investigate the effect of small-scale surface roughness on surface waves, ground reflectivity, and the significance of the incoherent scattered fields, an analytical solution based on perturbation theory is proposed. In this formulation, perturbation theory is applied to a volumetric integral equation for the induced polarisation current in the top rough layer of the dielectric interface. The perturbation parameter is the normalised rms height of the rough surface and an iterative solution starting from the unperturbed problem (dielectric half-space with smooth interface) is obtained. Basically, the formulation is similar to what has recently been applied to evaluate the far-field scattering from rough surfaces with inhomogeneous profiles when illuminated by a plane wave [2]. In Section 4,

the solution for dipole excitation is obtained by expanding the radiated field of the dipole in terms of a continuous spectrum of plane waves and adding the solution for each plane wave coherently. Statistical analysis is carried out analytically for characterising the coherent (mean) and incoherent (fluctuation) fields. The results are compared with the Sommerfeld solution and the depolarisation effects are investigated.

2 Polarisation current in a slightly rough surface

As mentioned earlier, the first step towards evaluating the field generated by an arbitrary dipole above a ground plane with a rough interface is to consider plane wave illumination. To obtain the scattered field, a perturbation solution to a volumetric integral equation for the induced polarisation current over the top rough layer of the surface is derived using a procedure similar to what is presented in [2]. Fig. 1 shows the geometry of the scattering problem where a dielectric half-space with an arbitrary dielectric profile and rough interface is illuminated by a plane wave from the upper medium. Suppose the surface height variation is small compared with the wavelength (λ) of the incident wave. The incident wave with an arbitrary polarisation \mathbf{Q} can be written as

$$\mathbf{E}^i(\vec{r}) = \mathbf{Q}e^{ik_0\hat{\mathbf{k}}^i \cdot \vec{r}}$$

where $k_0 = 2\pi/\lambda$ is the free space propagation constant, and $\hat{\mathbf{k}}^i$ is the unit vector along the direction of propagation, given by

$$\hat{\mathbf{k}}^i = \sin\theta_i \cos\phi_i \hat{\mathbf{x}} + \sin\theta_i \sin\phi_i \hat{\mathbf{y}} - \cos\theta_i \hat{\mathbf{z}} = \mathbf{k}_\perp^i/k_0 - \hat{\mathbf{z}}k_z^i$$

To make the solution tractable, the permittivity of the top layer down to a depth of d is considered to be uniform, where $-d < \min\{\text{surface profile}\}$. Denote the surface height profile by a function $z = \Delta f(x, y)$, where $f(x, y)$ is a zero-mean stationary random process with a known autocorrelation function and variance 1, and $\Delta \ll \lambda$ is a small constant known as the perturbation parameter. In the following derivation, it is assumed that the medium below the top layer is stratified, that is, the relative permittivity is only a function of z .

In the absence of the top homogeneous rough layer, the incident wave would be reflected at the smooth interface between the free space and the stratified half-space soil medium. This reflected wave can be expressed by

$$\mathbf{E}^r(\vec{r}) = \mathbf{E}^r(0)e^{ik_0\hat{\mathbf{k}}^r \cdot \vec{r}}$$

where $\hat{\mathbf{k}}^r$ is the direction of propagation of the reflected wave, given by

$$\hat{\mathbf{k}}^r = \hat{\mathbf{k}}^i - 2(\hat{\mathbf{z}} \cdot \hat{\mathbf{k}}^i)\hat{\mathbf{z}} = \mathbf{k}_\perp^i/k_0 + \hat{\mathbf{z}}k_z^i$$

and $\mathbf{E}^r(0)$ denotes the magnitude of the polarisation vector of the reflected wave, which can be obtained from

$$\mathbf{E}^r(0) = [r_v \hat{\mathbf{v}}_r \hat{\mathbf{v}}_i + r_h \hat{\mathbf{h}}_r \hat{\mathbf{h}}_i] \cdot \mathbf{Q}$$

Here, r_v and r_h are the Fresnel reflection coefficients, and the

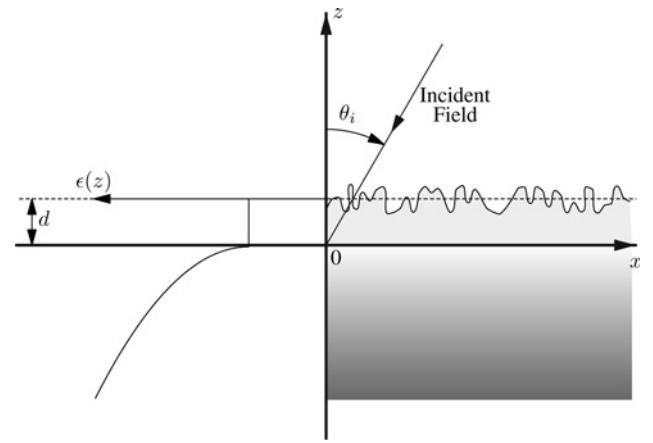


Fig. 1 Inhomogeneous half-space medium with a rough interface

Left side of this figure shows the dielectric profile

horizontal and vertical unit vectors are given by

$$\hat{\mathbf{h}}_s = \frac{\hat{\mathbf{k}}^s \times \hat{\mathbf{z}}}{|\hat{\mathbf{k}}^s \times \hat{\mathbf{z}}|}, \quad \hat{\mathbf{v}}_s = \hat{\mathbf{h}}_s \times \hat{\mathbf{k}}^s \quad (1)$$

where the subscript s can be i or r for the incident and reflected waves, respectively. In the presence of the homogeneous rough layer, the incident and reflected waves induce a polarisation current within the top dielectric layer, which is the source of the scattered field. The polarisation current in terms of the total field and the permittivity of the layer is

$$\mathbf{J}(\mathbf{r}) = -ik_0 Y_0 (\epsilon - 1) \mathbf{E}^t \quad (2)$$

where $Y_0 = 1/Z_0$ is the characteristic admittance of free space, and

$$\mathbf{E}^t = \mathbf{E}^i + \mathbf{E}^r + \mathbf{E}^s$$

The scattered field \mathbf{E}^s can, in turn, be expressed in terms of the polarisation current and is given by

$$\mathbf{E}^s = ik_0 Z_0 \int_{V_{\text{slab}}} \bar{\mathbf{G}}(\mathbf{r}, \mathbf{r}') \cdot \mathbf{J}(\mathbf{r}') d\mathbf{v}' \quad (3)$$

where $\bar{\mathbf{G}}(\mathbf{r}, \mathbf{r}')$ is the dyadic Green's function of the half-space stratified medium (in the absence of the top rough layer), and is given by [3] (see equation (4) on the bottom of the next page)

In (4), $k_z = \sqrt{k^2 - k_x^2 - k_y^2}$, $\mathbf{k}_\perp = k_x \hat{\mathbf{x}} + k_y \hat{\mathbf{y}}$ and $\hat{\mathbf{h}}(\pm k_z)$ and $\hat{\mathbf{v}}(\pm k_z)$ can be obtained from (1) with $\hat{\mathbf{k}}^s = (k_x \hat{\mathbf{x}} + k_y \hat{\mathbf{y}} \pm k_z \hat{\mathbf{z}})/k_0$.

Substituting (3) into (2), the following integral equation for the polarisation current can be obtained

$$\frac{1}{\epsilon - 1} \mathbf{J}(\mathbf{r}) = -ik_0 Y_0 (\mathbf{E}^i + \mathbf{E}^r) + k_0^2 \int_{-\infty}^{\infty} \int_0^{d+\Delta f(x', y')} \bar{\mathbf{G}}(\mathbf{r}, \mathbf{r}') \cdot \mathbf{J}(\mathbf{r}') d\mathbf{v}' \quad (5)$$

An approximate solution for the integral equation can be

obtained using a perturbation technique. The total polarisation current is expanded in terms of a perturbation series given by

$$\mathbf{J}(\mathbf{r}) = \sum_{n=0}^{\infty} \mathbf{J}_n(\mathbf{r})\Delta^n \quad (6)$$

with the expectation that $\lim_{n \rightarrow \infty} \mathbf{J}_n(\mathbf{r}) = 0$. The most inner integral in (5) is expanded into a power series in terms of Δ and then a recursive set of equations for \mathbf{J}_n are obtained. These currents are expressed in term of their two-dimensional Fourier transforms defined by

$$\mathbf{J}_n(\mathbf{r}) = \frac{1}{(2\pi)^2} \int d^2\mathbf{k}_{\perp} \tilde{\mathbf{J}}_n(\mathbf{k}_{\perp}, z) e^{i\mathbf{k}_{\perp} \cdot \bar{\rho}} \quad (7)$$

After much algebraic manipulation, the analytical solution for the induced polarisation current to any desired order is obtained [2]. The expression for $\tilde{\mathbf{J}}_0(\mathbf{k}_{\perp}, z)$ is given by

$$\tilde{\mathbf{J}}_0(\mathbf{k}_{\perp}, z) = (2\pi)^2 \delta(\mathbf{k}_{\perp} - \mathbf{k}_{\perp}^i) [J_{0h}(z) \hat{h}_i + J_{0t}(z) \hat{t}_i + J_{0z}(z) \hat{z}] \quad (8)$$

where $\hat{t}_i = \hat{z} \times \hat{h}_i$, and

$$\begin{aligned} J_{0h}(z) &= -i \frac{2k_0 k_z^i}{k_z^i + k_{1z}^i} Y_0(\epsilon - 1) C_0^h(k_{\rho}^i, z) [\mathbf{Q} \cdot \hat{h}_i] e^{-ik_z^i z} \\ J_{0t}(z) &= -i \frac{2k_0 k_z^i k_{1z}^i}{k_{\rho}^i (\epsilon k_z^i + k_{1z}^i)} Y_0(\epsilon - 1) C_0^v(k_{\rho}^i, z) [\mathbf{Q} \cdot \hat{z}] e^{-ik_z^i z} \\ J_{0z}(z) &= -i \frac{2k_0 k_z^i}{\epsilon k_z^i + k_{1z}^i} Y_0(\epsilon - 1) C_1^v(k_{\rho}^i, z) [\mathbf{Q} \cdot \hat{z}] e^{-ik_z^i z} \end{aligned} \quad (9)$$

The parameters used in these expressions for the zeroth-order current are given by

$$\begin{aligned} k_{1z}^i &= k_0 \sqrt{\epsilon - \sin^2 \theta_i}, \quad k_{\rho}^i = k_0 \sin \theta_i, \\ R_h^i &= \frac{k_z^i - k_{1z}^i}{k_z^i + k_{1z}^i}, \quad R_v^i = \frac{\epsilon k_z^i - k_{1z}^i}{\epsilon k_z^i + k_{1z}^i} \\ C_n^h(k_{\rho}, z) &= \frac{(-1)^n (R_h - r_h) e^{ik_{1z} z} + (R_h r_h - 1) e^{-ik_{1z} z}}{R_h (R_h - r_h) e^{ik_{1z} z} + (R_h r_h - 1) e^{-ik_{1z} z}} \\ C_n^v(k_{\rho}, z) &= \frac{(-1)^n (r_v - R_v) e^{ik_{1z} z} + (R_v r_v - 1) e^{-ik_{1z} z}}{R_v (R_v - r_v) e^{ik_{1z} z} + (R_v r_v - 1) e^{-ik_{1z} z}} \end{aligned}$$

As before, r_h and r_v denotes the Fresnel reflection coefficients of the half-space medium. If the half-space dielectric is homogeneous ($r_h = R_h$ and $r_v = R_v$), the values of C_n^h and C_n^v are one. The expressions for the first-order currents are similar to those of the zeroth order, and are given in the Appendix.

3 Evaluation of scattered fields

Substituting the expressions for polarisation currents into (3), and following a similar procedure which resulted in (6) of [2], the scattered field to the N th order in Δ is obtained

$$\begin{aligned} E^s(\mathbf{r}, \hat{\mathbf{k}}^i) &= \frac{ik_0 Z_0}{(2\pi)^2} \int d^2\mathbf{k}_{\perp} \left\{ \int_0^d \tilde{\mathbf{G}}(\mathbf{k}_{\perp}; z, z') \cdot \tilde{\mathbf{J}}(\mathbf{k}_{\perp}, z') dz' \right. \\ &+ \sum_{n=0}^{N-1} \sum_{m=0}^n \frac{\binom{n}{m} \Delta^{n+1}}{(n+1)!} \cdot \frac{\partial^m}{\partial z'^m} \tilde{\mathbf{G}}(\mathbf{k}_{\perp}; z, d) \\ &\cdot \left[\frac{\partial^{n-m}}{\partial z'^{n-m}} \tilde{\mathbf{J}}(\mathbf{k}_{\perp}, d) * \otimes F(\mathbf{k}_{\perp}) \right] \end{aligned} \quad (10)$$

where

$$\begin{aligned} \tilde{\mathbf{G}}(\mathbf{k}_{\perp}; z, z') &= \frac{i}{2} \left\{ \hat{h}(k_z) \left[r_h \hat{h}(-k_z) e^{ik_z z'} + \hat{h}(k_z) e^{-ik_z z'} \right] \right. \\ &+ \hat{v}(k_z) \left[r_v \hat{v}(-k_z) e^{ik_z z'} + \hat{v}(k_z) e^{-ik_z z'} \right] \left. \right\} e^{ik_z z}, \quad \text{if } z > z' \end{aligned} \quad (11)$$

which is the Fourier transformation of the dyadic Green's function.

Equation (10) can be divided into two parts

$$E^s(\mathbf{r}, \hat{\mathbf{k}}^s, \hat{\mathbf{k}}^i) = E^{sf}(\mathbf{r}, \hat{\mathbf{k}}^r, \hat{\mathbf{k}}^i) + E^{sr}(\mathbf{r}, \hat{\mathbf{k}}^s, \hat{\mathbf{k}}^i) \quad (12)$$

$E^{sf}(\mathbf{r}, \hat{\mathbf{k}}^r, \hat{\mathbf{k}}^i)$ is the scattered field to the zeroth order in Δ . Substituting the zeroth-order currents (9) into (10), the zeroth-order field is given by

$$\begin{aligned} E_{PQ}^{sf}(\mathbf{r}, \hat{\mathbf{k}}^r, \hat{\mathbf{k}}^i) &= e^{ik_0 \hat{\mathbf{k}}^r \cdot \mathbf{r}} \mathbf{P} \cdot \left\{ \hat{h}(k_z^i) \hat{h}(-k_z^i) R_h^{(0)}(k_{\rho}^i) \right. \\ &+ \hat{v}(k_z^i) \hat{v}(-k_z^i) R_v^{(0)}(k_{\rho}^i) \left. \right\} \cdot \mathbf{Q} \end{aligned} \quad (13)$$

where \mathbf{Q} and \mathbf{P} are the polarisation vectors of the incident and scattered fields, respectively, and

$$\begin{aligned} R_h^{(0)}(k_{\rho}^i) &= \left[(1 + R_h^i) C_0^h(k_{\rho}^i, d) - 1 \right] e^{-2ik_z^i d} \\ R_v^{(0)}(k_{\rho}^i) &= \left[(1 + R_h^i) C_0^h(k_{\rho}^i, d) - 1 \right] e^{-2ik_z^i d} \end{aligned} \quad (14)$$

The zeroth-order solution is equivalent to the reflected field from the original multi-layer medium with a flat interface ($f(x, y) = 0$), and the expressions in (14) give the total reflection coefficients at the air-medium interface. It should be noted that $(\hat{v}(-k_z^i), \hat{h}(-k_z^i)) = (\hat{v}_i, \hat{h}_i)$ and

$$\tilde{\mathbf{G}}(\mathbf{r}, \mathbf{r}') = -\hat{z} \hat{z} \frac{\delta(\mathbf{r} - \mathbf{r}')}{k_0^2} + \frac{i}{8\pi^2} d^2 \mathbf{k}_{\perp} \frac{e^{i\mathbf{k}_{\perp} \cdot (\bar{\rho} - \bar{\rho}')}}}{k_z} \left\{ \begin{aligned} &\left\{ \left[r_h \hat{h}(k_z) e^{ik_z z} + \hat{h}(-k_z) e^{-ik_z z} \right] \hat{h}(-k_z) \right. \\ &+ \left. \left[r_v \hat{v}(k_z) e^{ik_z z} + \hat{v}(-k_z) e^{-ik_z z} \right] \hat{v}(-k_z) \right\} e^{ik_z z'}, \quad \text{if } z < z' \\ &\left\{ \hat{h}(k_z) \left[r_h \hat{h}(-k_z) e^{ik_z z'} + \hat{h}(k_z) e^{-ik_z z'} \right] \right. \\ &+ \left. \hat{v}(k_z) \left[r_v \hat{v}(-k_z) e^{ik_z z'} + \hat{v}(k_z) e^{-ik_z z'} \right] \right\} e^{ik_z z}, \quad \text{if } z > z' \end{aligned} \right. \quad (4)$$

$(\hat{v}(k_z^i), \hat{h}(k_z^i)) = (\hat{v}_r, \hat{h}_r)$. The superscript ‘f’ in (13) denotes the flat interface.

$E^{sr}(\mathbf{r}, \hat{\mathbf{k}}^s, \hat{\mathbf{k}}^i)$ is the higher-order scattered field, which only exists when the surface is rough. Substituting the polarisation currents into (10), and after some algebraic manipulations, the following expression for the scattered field is obtained (see (15))

Note that (15) is valid for all points $z > d$, including observation points very close to the surface. In the special case where the observation point is far from the surface ($z \gg d$), the stationary phase approximation can be used for evaluating the integral in (15). The far-field expansion for the scattered field can be written in terms of a scattering matrix which depends on the direction of observation. Comparing (15) with (14) and (15) in [2], E_{PQ}^{sr} can be expressed in terms of scattering matrix elements (see (16))

where the scattering matrix elements in (16) are given in [2]. The near-field expression in (16) can be interpreted as the superposition of the scattered fields from all different directions denoted by \mathbf{k} . The integrand corresponding to $|\mathbf{k}_\perp| < k_0$ can be interpreted as the upward propagating waves emanating from the surface. When $|\mathbf{k}_\perp| > k_0$, the corresponding waves are non-propagating, which are known as the surface wave whose contributions are confined to the vicinity of the interface. It should be emphasised that the quantities of interest are the statistical mean and the standard deviation of the scattered field. These surface waves are caused by the rough surface scattering and do not exist when the surface is flat.

Performing the ensemble averaging of (12), it is found that, up to the second order

$$\langle E^s(\mathbf{r}, \hat{\mathbf{k}}^r, \hat{\mathbf{k}}^i) \rangle \simeq E^{sf}(\mathbf{r}, \hat{\mathbf{k}}^r, \hat{\mathbf{k}}^i) + \langle E^{sr(2)}(\mathbf{r}, \hat{\mathbf{k}}^r, \hat{\mathbf{k}}^i) \rangle \quad (17)$$

Here, $\langle E^{sr(2)}(\mathbf{r}, \hat{\mathbf{k}}^r, \hat{\mathbf{k}}^i) \rangle$, like $E^{sf}(\mathbf{r}, \hat{\mathbf{k}}^r, \hat{\mathbf{k}}^i)$ in (13), can be

expressed as (see (18))

where $R_h^{(2)}(k_\rho^i)$ and $R_v^{(2)}(k_\rho^i)$ are also given in the Appendix. Since $f(x, y)$ is a zero-mean Gaussian process, it can be shown that the average of odd-order fields vanish. The next term of the coherent field is the fourth-order E^{sr} , which will be ignored because of the assumption of the slight roughness.

For the evaluation of the incoherent scattering power (variance of the field), only the first-order scattered field is retained. Re-arranging (16), we have

$$E_{PQ}^{sr}(\mathbf{r}, \hat{\mathbf{k}}^s, \hat{\mathbf{k}}^i) = \frac{i}{2\pi} \int d^2 \mathbf{k}_\perp I_{PQ}(\mathbf{k}_\perp, \mathbf{k}_\perp^i) \Delta F(\mathbf{k}_\perp - \mathbf{k}_\perp^i) \quad (19)$$

where $I_{PQ}(\mathbf{k}_\perp, \mathbf{k}_\perp^i)$ is given by (see (20))

Noting that

$$\begin{aligned} \Delta^2 \langle F(\mathbf{k}_\perp) F^*(\mathbf{k}_\perp^i) \rangle &= \Delta^2 \langle F(\mathbf{k}_\perp) F(-\mathbf{k}_\perp^i) \rangle \\ &= (2\pi)^2 \delta(\mathbf{k}_\perp - \mathbf{k}_\perp^i) W(\mathbf{k}_\perp) \end{aligned} \quad (21)$$

the incoherent scattering power, up to the second order in Δ , is given by

$$\begin{aligned} \langle |E_{PQ}^s - \langle E_{PQ}^s \rangle|^2 \rangle &\simeq \langle |E_{PQ}^{sr(1)}|^2 \rangle \\ &= \Delta^2 \int d^2 \mathbf{k}_\perp |I_{PQ}(\mathbf{k}_\perp, \mathbf{k}_\perp^i)|^2 W(\mathbf{k}_\perp - \mathbf{k}_\perp^i) \end{aligned} \quad (22)$$

As mentioned previously, (16) is expressed as a continuous spectrum of scattered plane waves. What is expressed mathematically by (21) indicates that these plane waves are mutually uncorrelated. Therefore (22) is simply the

$$\begin{aligned} E_{PQ}^{sr}(\mathbf{r}, \hat{\mathbf{k}}^s, \hat{\mathbf{k}}^i) &= \frac{-k_0 Z_0}{8\pi^2} \sum_{N=1}^{\infty} \Delta^N \int d^2 \mathbf{k}_\perp \frac{e^{i\mathbf{k}_\perp \cdot \bar{\rho} + ik_z(z-d)}}{k_z} \sum_{n=0}^{N-1} \sum_{m=0}^{N-n-1} \frac{\binom{N-n-1}{m} (ik_z)^m}{(N-n)!} \\ &\quad \times \mathbf{P} \cdot \{ \hat{h}(k_z) \hat{h}(k_z) [R_h + (-1)^m] C_m^h(k_\rho, d) + \hat{v}(k_z) \hat{i}(k_z) [R_v^s - (-1)^m] C_m^v(k_\rho, d) \frac{k_z}{k_0} \\ &\quad + \hat{v}(k_z) \hat{z} [R_v + (-1)^m] C_{m+1}^v(k_\rho, d) \frac{k_\rho}{k_0} \} \cdot \left[\left(\frac{\partial^{N-n-m-1}}{\partial(z)^{N-n-m-1}} \tilde{\mathcal{J}}_n(\mathbf{k}_\perp, d) \right) * \otimes^{N-n} F(\mathbf{k}_\perp) \right] \end{aligned} \quad (15)$$

$$\begin{aligned} E_{PQ}^{sr}(\mathbf{r}, \hat{\mathbf{k}}^s, \hat{\mathbf{k}}^i) &= \frac{i}{2\pi} \sum_{N=1}^{\infty} \int d^2 \mathbf{k}_\perp \frac{e^{i\mathbf{k} \cdot \mathbf{r}}}{k_z} \mathbf{P} \cdot \{ \hat{h}(k_z) \hat{h}(-k_z^i) S_{hh}^{(N)}(\mathbf{k}, \mathbf{k}_i) + \hat{h}(k_z) \hat{v}(-k_z^i) S_{hv}^{(N)}(\mathbf{k}, \mathbf{k}_i) + \hat{v}(k_z) \hat{h}(-k_z^i) S_{vh}^{(N)}(\mathbf{k}, \mathbf{k}_i) \\ &\quad + \hat{v}(k_z) \hat{v}(-k_z^i) S_{vv}^{(N)}(\mathbf{k}, \mathbf{k}_i) \} \cdot \mathbf{Q} \end{aligned} \quad (16)$$

$$\langle E^{sr(2)}(\mathbf{r}, \hat{\mathbf{k}}^r, \hat{\mathbf{k}}^i) \rangle = e^{i\mathbf{k}_0 \hat{\mathbf{k}}^r \cdot \mathbf{r}} \mathbf{P} \cdot \left\{ \hat{h}(k_z^i) \hat{h}(-\hat{k}_z^i) R_h^{(2)}(k_\rho^i) + \hat{v}(k_z^i) \hat{v}(-\hat{k}_z^i) R_v^{(2)}(k_\rho^i) \right\} \cdot \mathbf{Q} \quad (18)$$

$$\begin{aligned} I_{PQ}(\mathbf{k}_\perp, \mathbf{k}_\perp^i) &= \frac{e^{i\mathbf{k} \cdot \mathbf{r}}}{k_z \Delta F(\mathbf{k}_\perp - \mathbf{k}_\perp^i)} \mathbf{P} \cdot \{ \hat{h}(k_z) \hat{h}(-k_z^i) S_{hh}^{(1)}(\mathbf{k}, \mathbf{k}_i) + \hat{h}(k_z) \hat{v}(-k_z^i) S_{hv}^{(1)}(\mathbf{k}, \mathbf{k}_i) \\ &\quad + \hat{v}(k_z) \hat{h}(-k_z^i) S_{vh}^{(1)}(\mathbf{k}, \mathbf{k}_i) + \hat{v}(k_z) \hat{v}(-k_z^i) S_{vv}^{(1)}(\mathbf{k}, \mathbf{k}_i) \} \cdot \mathbf{Q} \end{aligned} \quad (20)$$

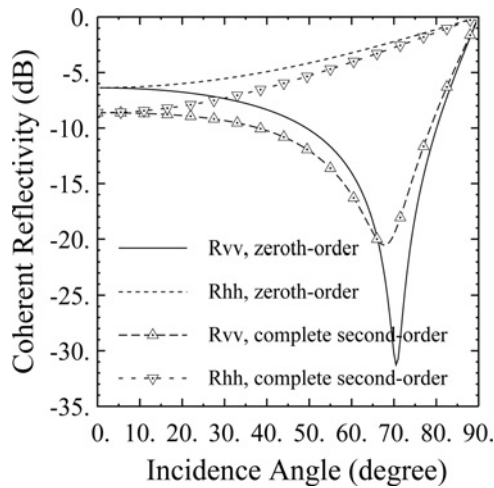


Fig. 2 Magnitude of the reflection coefficients in (14) against incidence angle

The underlying ground is homogeneous, and the dielectric constant is $\epsilon = 8 + i1$. The simulation frequency is 890 MHz at which the surface roughness parameters are $ks = 0.3$ and $kl = 3.0$

integration of the power carried by each plane wave. For observation points near the surface, (22) must be carried out numerically and cannot be simplified any further. The convergence of the integral can be examined noting that $W(\mathbf{k}_\perp)$ decreases as $|\mathbf{k}_\perp|$ increases and the fact that for $|\mathbf{k}_\perp| > k_0$, k_z becomes pure imaginary which causes the integrand $(|I_{PQ}(\mathbf{k}_\perp, \mathbf{k}_\perp^i)|^2)$ to decay rapidly.

To demonstrate the effect of the surface roughness on the surface reflectivity, a numerical example is considered. Both coherent reflectivity and incoherent reflectivity $(\langle |E_{PQ}^{sr(1)}|^2 \rangle / |E^i|^2)$ as a function of observation point height are calculated. These plane wave illumination examples simulate a situation where the transmitter (receiver) is airborne and the receiver (transmitter) is near the rough interface. Consider a rough soil surface with rms height of 0.016 m, correlation length 0.16 m and dielectric constant $\epsilon = 8 + i1$ illuminated by a plane wave generated by a source operating at $f = 890$ MHz. At this frequency, the

normalised rms height and correlation length are, respectively, $ks = 0.3$ and $kl = 3.0$. Fig. 2 shows the magnitude of the zeroth-order and complete second-order mean field in (14) against incidence angle. In this simulation, the correlation function for the rough surface is assumed Gaussian. The complete second-order solution demonstrates the effect of surface roughness on the surface reflectivity. Basically, the surface roughness reduces the surface reflectivity and causes a slight shift in the Brewster angle.

It should be noted that the formulation of the second-order coherent reflection coefficients in (18) does not converge for surfaces with an exponential correlation function. This may be because of the fact that higher-order terms are excluded. However, this problem is not observed in the formulation for the incoherent wave. Figs. 3a and b show comparisons between the zeroth-order coherent and incoherent reflectivities as a function of the height of the observation point for an exponential correlation function. It is shown that for vertical polarisation and observation point heights $< 0.1\lambda$, the incoherent reflectivity is significant and dominant near the Brewster angle. However, for horizontal polarisation, independent of the incidence angle, the incoherent reflectivity is much smaller than the coherent reflectivity.

Generally, the incoherent reflectivities decrease as the incidence angle decreases. This could be qualitatively explained by use of the Rayleigh criterion [4]. The criterion is stated as follows: for a surface characterised by a distribution of irregularities of height h , if h satisfies

$$h \leq \frac{\lambda}{16 \cos \theta} \quad (23)$$

where θ is the incidence angle, the surface can be considered smooth. As the incidence angle increase, the surface appears 'more flat'. Therefore the incoherent scattering decreases.

The same is true for the coherent field as shown in Fig. 2, where the coherent reflectivity approaches unity when θ is increased to 90° .

It is noted that the incoherent reflectivities vary as the height of the observation point changes. As mentioned previously, the scattered field can be decomposed into two components: upward propagating waves and surface waves. When the

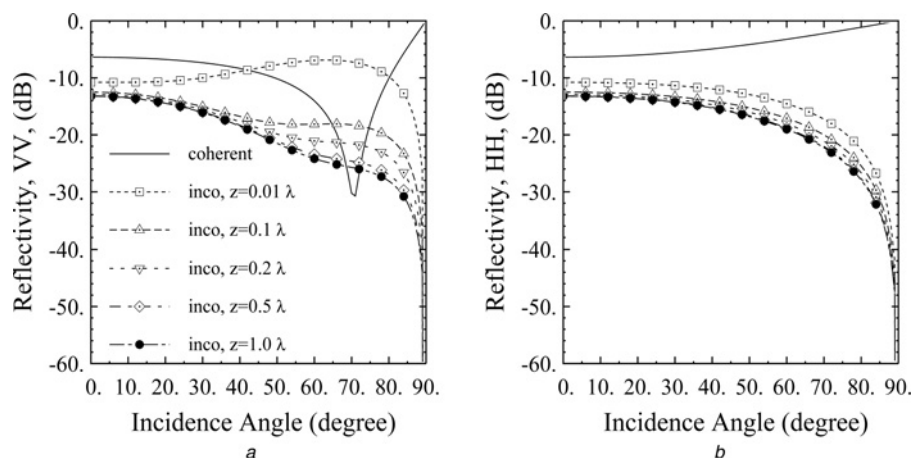


Fig. 3 Comparison between the coherent and incoherent reflectivities against incidence angle

The underlying ground is homogeneous, and $\epsilon = 8 + i1$, and the rough surface has exponential correlation function, $ks = 0.3$, and $kl = 3.0$. The incoherent reflectivities are plotted for different observation point heights

a vv
b hh

height increases, while the surface wave components attenuate, the propagating waves remain unattenuated. This phenomenon is demonstrated in Fig. 4 where the integrand of (19) is plotted in k_{\perp} space. The normalised magnitude of the integrand is shown in grey scale over an area with the radius of $2k_o$ in the spectral domain. The propagating waves are confined in a circle of radius k_o , whereas the surface waves are outside the k_o circle. Figs 4a and d show the incoherent vv- and hh-polarised power spectral densities for an observation point 0.01λ above the rough surface when the incidence angle is 20° . The integrand is normalised with respect to the value at $(k_x, k_y) = (k_o \sin 18.8^\circ, 0.0)$ for vv-polarisation and $(k_o \sin 21.2^\circ, 0.0)$ for hh-polarisation. In this case, most of the power is in the k_o circle, which justifies the lack of sensitivity of the incoherent reflectivity to the height variation at 20° shown in Figs. 5a and b. Figs. 4b and e, respectively, show the incoherent vv- and hh-polarised power spectral densities when the observation point is 0.01λ above the rough surface at incidence angle 80° . The integrand is normalised with respect to the value at $(k_x, k_y) = (-k_o, 0.0)$ for vv-polarisation and $(k_o, 0.0)$ for hh-polarisation. A significant component of incoherent scattering is from the contribution of the surface waves (the area outside the k_o circle). It is also noticed that, for vv-polarisation, incoherent scattering is mostly from the waves around the backscattering direction. As the height of the observation point increases to 0.5λ , the contribution from the surface waves almost vanishes, as shown in Figs. 5c and f.

In the near-field region, all field components are present in general. Decomposing the field components into v , h and k

components, the behaviour of the cross-polarised incoherent scattered waves are demonstrated next. Figs. 5a–d show the incoherent cross-polarised scattering, including vh-, hv-, kv- and kh-polarisations. Like the co-polarised scattering, the cross-polarised incoherent scattered power is stronger for observation points close to the surface. Also, for a v-polarised incident field, the cross-polarised scattering powers are stronger than those of the h-polarised incident field.

4 Evaluation of field of a short dipole above a rough surface

Another problem of practical importance is the characterisation of the field of a short dipole above a rough surface. Consider an infinitesimal current element given by $\mathbf{Q}\delta(\mathbf{r}-\mathbf{r}')$ where \mathbf{Q} denotes the polarisation of the dipole antenna, and \mathbf{r}' represents the location of the dipole. At the observation point, \mathbf{r} , the direct radiated field from the dipole is given by [5]

$$\mathbf{E}^d(\mathbf{r}, \mathbf{r}') = \frac{iZ_o}{4\pi k_o} \left\{ \left[\frac{-1 + ik_o R + k_o^2 R^2}{R^3} \right] \mathbf{Q} + \left[\frac{3 - 3ik_o R - k_o^2 R^2}{R^5} \right] (\mathbf{Q} \cdot \mathbf{R}) \mathbf{R} \right\} \quad (24)$$

where $\mathbf{R} = \mathbf{r} - \mathbf{r}'$ and $R = |\mathbf{R}|$. For $z < z'$, (24) can be expressed in terms of an integral of plane waves given by

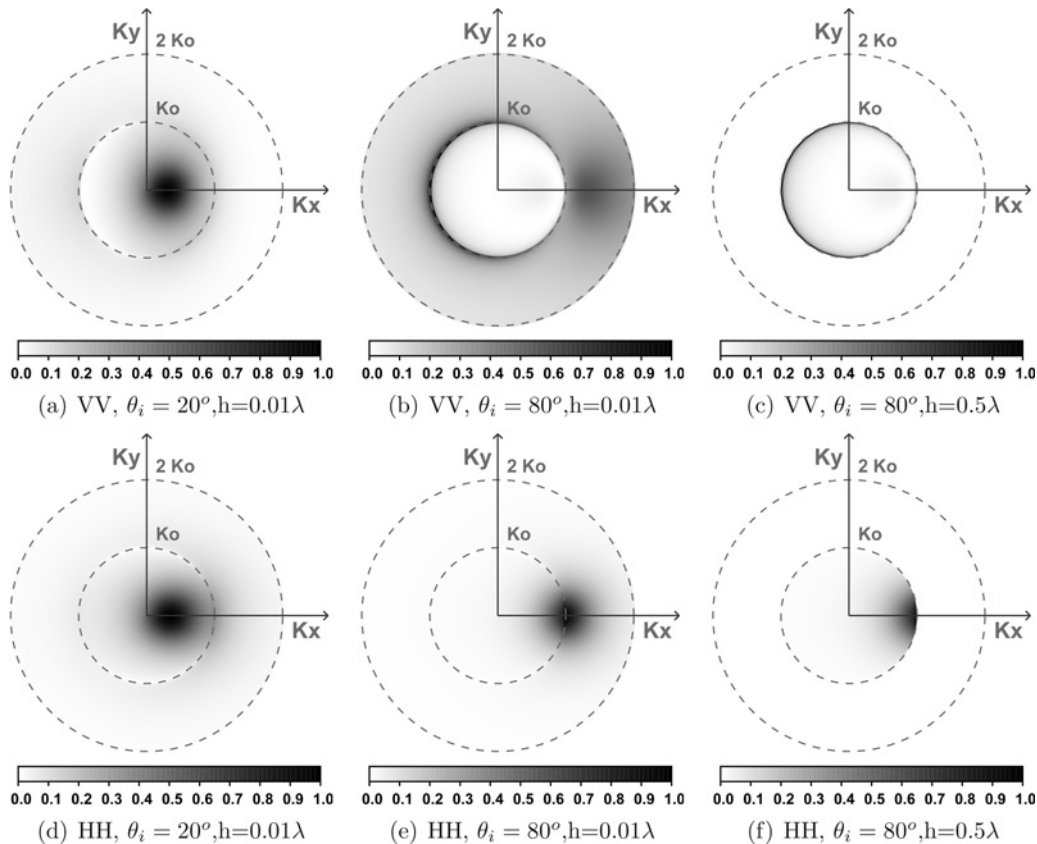


Fig. 4 Spectral distribution of the incoherent scattered power generated from the rough surface

a and d For vv- and hh-polarisation, respectively, at the incidence angle 20° , and the height is 0.01λ
 b and e For vv- and hh-polarisation, respectively, at the incidence angle 80° , and the height is 0.01λ
 c and f Same as (b) and (e), but the height is 0.5λ

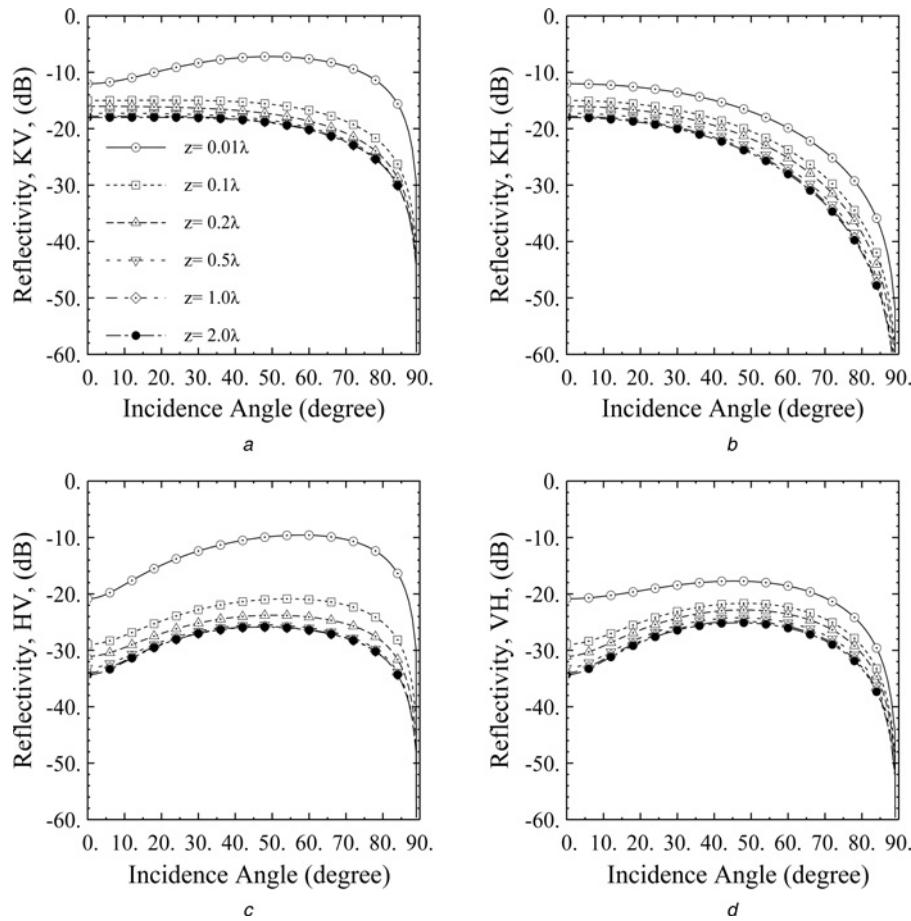


Fig. 5 Cross-polarised incoherent scattered fields against incidence angle

a kv
b kh
c hv
d vh

The incoherent reflectivities are plotted for different observation point heights

$$\mathbf{E}^d(\mathbf{r}, \mathbf{r}') = \frac{-k_o Z_o}{8\pi^2} \int d^2 \mathbf{k}_\perp \frac{e^{i\mathbf{k}_\perp \cdot (\hat{\rho} - \hat{\rho}')}}{k_z} \times [\hat{h}(-k_z)\hat{h}(-k_z) + \hat{v}(-k_z)\hat{v}(-k_z)] \cdot \mathbf{Q} e^{-ik_z(z-z')} \quad (25)$$

The mean field can be obtained by evaluating the integral of the mean fields corresponding to each individual plane wave and is given by

$$\langle E_{PQ}^g(\mathbf{r}, \mathbf{r}') \rangle = \frac{-k_o Z_o}{8\pi^2} \int d^2 \mathbf{k}_\perp \frac{e^{-i\mathbf{K} \cdot \mathbf{r}'}}{k_z} E_{PQ}^{sf}(\mathbf{r}, \hat{\mathbf{k}}, \hat{\mathbf{K}}) \quad (26)$$

where $\mathbf{k} = \mathbf{k}_\perp + k_z \hat{\mathbf{z}}$, and $\mathbf{K} = \mathbf{k}_\perp - k_z \hat{\mathbf{z}}$. Substituting (13) into (26), it is found that (see (27))

Equation (27) is obtained by noting that the reflection coefficients are azimuthally symmetric and therefore the integration with respect to ϕ is carried out analytically with the result expressed in terms of $P_Q^h(k_\rho)$ and $P_Q^v(k_\rho)$, which

are given in (33) and (34), respectively. The integral in (27) is a Sommerfeld type. When both \mathbf{r} and \mathbf{r}' are close to the ground and far from each other, the first term on the right-hand side, which can be viewed as the negative image source, dominates. This results in destructive interference with the direct wave, and hence the surface waves, which are accounted for in the integral of (27), become dominant. The integral in (27) can also be written in terms of asymptotic expressions available in the literature [6]. The numerical technique for the evaluation of the Sommerfeld integral is not discussed here. Interested readers are referred to [7]. Here, the objective is to investigate the significance of the rough surface which is included in the integral in (27) and in the incoherent scattered field.

The first-order incoherent scattered field is written in terms of a superposition of incoherent scattered fields

$$E_{PQ}^{g(1)}(\mathbf{r}, \mathbf{r}') = \frac{-k_o Z_o}{8\pi^2} \int d^2 \mathbf{k}_\perp \frac{e^{-i\mathbf{K} \cdot \mathbf{r}'}}{k_z} E_{PQ}^{sr(1)}(\mathbf{r}, \hat{\mathbf{k}}, \hat{\mathbf{K}}) \quad (28)$$

$$\langle E_{PQ}^g(\mathbf{r}, \mathbf{r}') \rangle = -\mathbf{P} \cdot \mathbf{E}^d(\mathbf{r}, 2(d-z')\hat{\mathbf{z}} + \mathbf{r}') + \frac{-k_o Z_o}{8\pi^2} \int_0^\infty k_\rho dk_\rho \frac{e^{ik_z(z+z')}}{k_z} \left\{ (1 + R_h) C_0^h(k_\rho, d) e^{-2ik_z d} P_Q^h(k_\rho) + (1 + R_v) C_0^v(k_\rho, d) e^{-2ik_z d} P_Q^v(k_\rho) \right\} \quad (27)$$

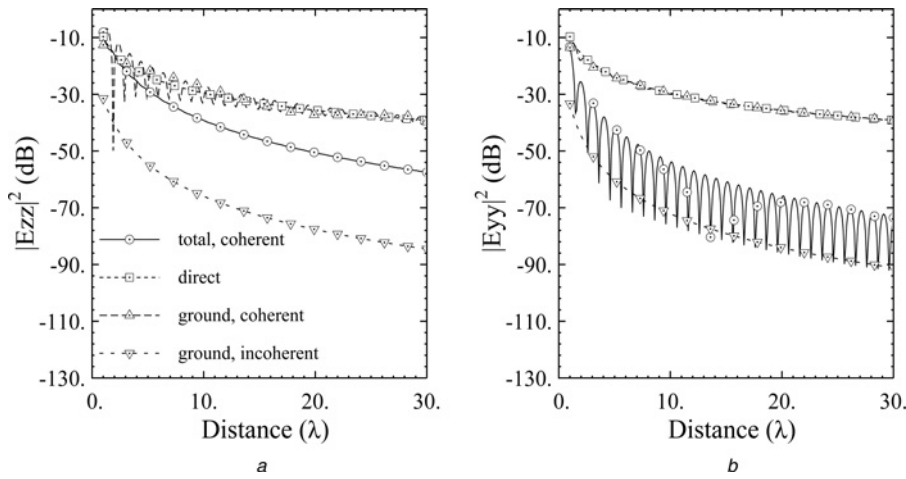


Fig. 6 Electric field against the distance between the source and observation point

The underlying ground is homogeneous ($\epsilon = 8 + i1$). The rough surface has an exponential correlation function, $ks = 0.3$, and $kl = 3.0$

a $\mathbf{Q} = \mathbf{P} = \hat{z}$
 b $\mathbf{Q} = \mathbf{P} = \hat{y}$

from which the incoherent scattered power is obtained and given by (see (29))

Note that the integral in (29) is 6-fold which is extremely difficult to evaluate numerically. Practically, the distance between the dipole and the observation point is large, which can be used to simplify (29). Suppose $\mathbf{r} = z\hat{z}$ and $|\mathbf{r}'| \gg \lambda$. Using the stationary phase approximation to evaluate the integrals on \mathbf{k}'_{\perp} and \mathbf{k}''_{\perp} , the incoherent scattering power can be obtained from (see (30))

Numerical simulations have been performed to demonstrate the effect of the surface roughness. Consider the rough surface of the previous example with parameters $\epsilon = 8 + i1$, $ks = 0.3$, $kl = 3.0$, and an exponential correlation function. Suppose the infinitesimal current source is placed at 0.2λ above the surface at a location $\mathbf{r}' = x'\hat{x}' + y'\hat{y}' + 0.2\lambda\hat{z}'$, and the observation point is at $(0, 0, 0.2\lambda)$. Figs. 6a ($\mathbf{Q} = \mathbf{P} = \hat{z}$) and 6b ($\mathbf{Q} = \mathbf{P} = \hat{y}$) show different components comprising the received power against the radial distance ($\sqrt{x'^2 + y'^2}$) between the current source and the observation point. It is shown that, as the distance increases, the reflection coefficients approach -1 , and the coherent ground contribution cancels the direct wave. The cancellation of the direct wave and the reflected wave for near-ground source and observation points results in the well-known field decay with distance behaviour of $1/r^2$ as shown in Fig. 6. Note that as the incidence angle approaches 90° , the effect of the surface roughness on the coherent field becomes insignificant, as explained previously when stating the Rayleigh criterion. In this circumstance, the dominant propagation mechanism is the coherent and incoherent surface waves. H-polarised surface

waves attenuate rapidly [8]. Therefore, in Fig. 6b, the surface wave is less significant than that in Fig. 6a, and the total field shows obvious interference phenomenon between the direct wave and reflected wave. The incoherent rough surface scattering is found to be more significant for horizontal polarisation. The effect for horizontal polarisation becomes more significant when the height of the observation point, the source, or both are lowered.

In the next simulation, the distance between source and observation point is fixed at 20λ , but the source point is moved on a circle of radius 20λ in the $x-z$ plane, as shown in Fig. 7. As before, the observation point is at $(0, 0, 0.2\lambda)$. However, the source is at $(20\lambda \sin\theta, 0, 0.2\lambda + 20\lambda \cos\theta)$ with $\theta \in [0^\circ, 90^\circ]$. Fig. 8a shows the coherent and

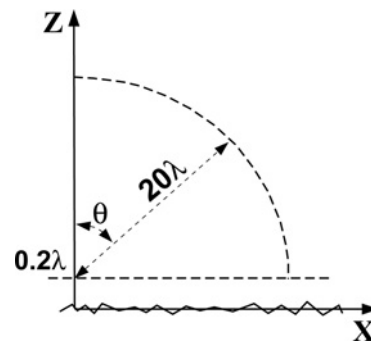


Fig. 7 Distance between the source and observation point is fixed at 20λ , but the source point is moved on a circle of radius 20λ in the $x-z$ plane

The observation point is at $(0, 0, 0.2\lambda)$, and the source is at $(20\lambda \sin \theta, 0, 0.2\lambda + 20\lambda \cos \theta)$ with $\theta \in [0^\circ, 90^\circ]$

$$\langle |E_{PQ}^{g(1)}(\mathbf{r}, \mathbf{r}')|^2 \rangle = \frac{k_0^2 Z_0^2}{64 \pi^4} \iint d^2 \mathbf{k}'_{\perp} d^2 \mathbf{k}''_{\perp} \frac{e^{i[(\mathbf{K}'')^* - \mathbf{K}'] \cdot \mathbf{r}'}}{k'_z (k''_z)^*} \int d^2 \mathbf{k}_{\perp} I_{PQ}(\mathbf{k}_{\perp}, \mathbf{k}'_{\perp}) I_{PQ}^*(\mathbf{k}_{\perp} + \mathbf{k}''_{\perp} - \mathbf{k}'_{\perp}, \mathbf{k}''_{\perp}) W(\mathbf{k}_{\perp} - \mathbf{k}'_{\perp}) \quad (29)$$

$$\langle |E_{PQ}^{g(1)}(\mathbf{r}, z'\hat{z})|^2 \rangle \simeq \frac{k_0^2 Z_0^2}{8 \pi^2 |\mathbf{r}|^2} \int d^2 \mathbf{k}_{\perp} \left| I_{PQ} \left(\mathbf{k}_{\perp}, -k_0 \frac{\rho \hat{\rho}}{|\mathbf{r}|} \right) \right|^2 W \left(\mathbf{k}_{\perp} + k_0 \frac{\rho \hat{\rho}}{|\mathbf{r}|} \right) \quad (30)$$

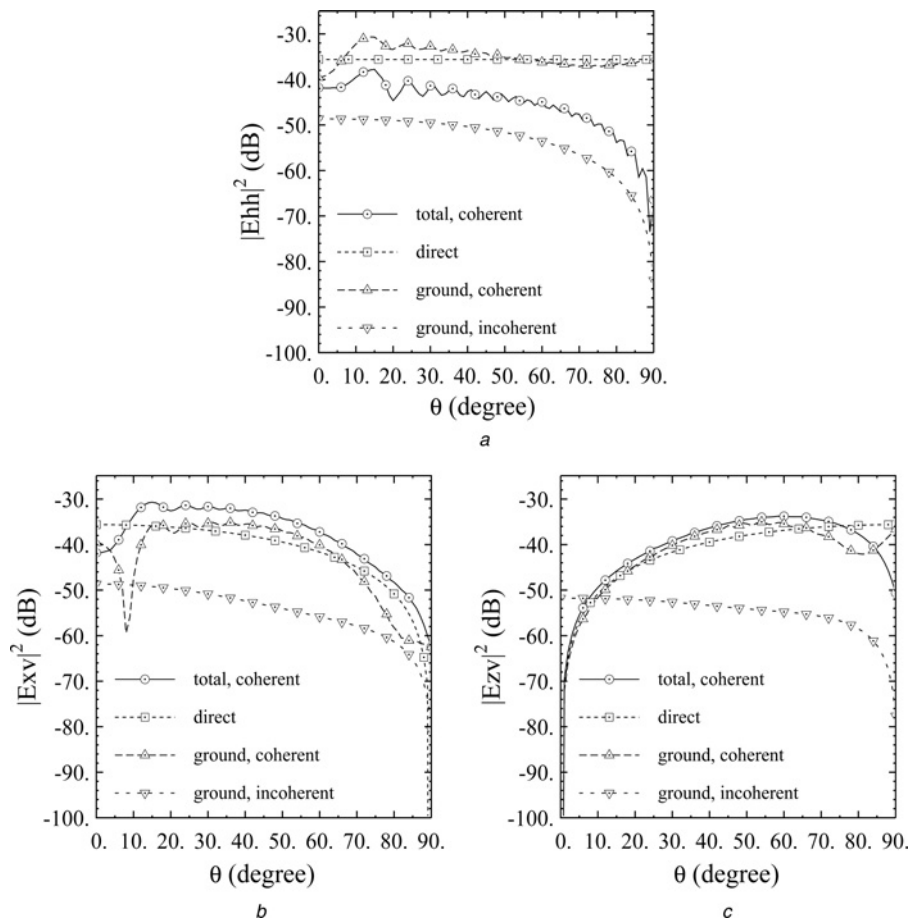


Fig. 8 Components of the received power as a function of the transmitter height for a fixed distance (20λ) between the transmitter and receiver

The observation point is at $(0, 0, 0.2\lambda)$, and the source is at $(20\lambda \sin\theta, 0, 0.2\lambda + 20\lambda \cos\theta)$

a $\mathbf{Q} = \mathbf{P} = \hat{h} = \hat{y}$

b and c $\mathbf{Q} = \hat{v} = (-\sin\theta, 0, \cos\theta)$, $\mathbf{P} = \hat{x}$ and $\mathbf{P} = \hat{z}$, respectively

incoherent powers with $\mathbf{Q} = \mathbf{P} = \hat{h} = \hat{y}$. When θ approaches 90° , the direct field and ground reflected field interfere with each other destructively, but the total coherent field is still about 10 dB higher than the incoherent field. In Figs. 8b and c, choosing $\mathbf{Q} = \hat{v} = (-\sin\theta, 0, \cos\theta)$ and $\mathbf{P} = \hat{x}$ for Fig. 8b and $\mathbf{P} = \hat{z}$ for Fig. 8c, show the components of the received power. Note that in both simulations, the polarisations at the observation point are not suitable to receive the ground reflected waves, which should be $(\sin\theta, 0, \cos\theta)$. Thus, the direct field dominates. When \mathbf{Q} and \mathbf{P} become perpendicular to each other, the coherent field diminishes, and the incoherent field becomes significant.

5 Conclusions

The radiation of a short electric dipole above a slightly rough surface is studied. This investigation is a natural extension of the classical Sommerfeld problem with the exception of the random surface irregularities at the interface between the two dielectric media. In this paper, the formulation for the near scattered field from a slightly rough surface when illuminated by plane waves is developed first. A perturbation technique is applied to solve the integral equation for the induced polarisation current. Analytical expressions for the coherent field (mean field) and incoherent scattered power at an arbitrary observation point, including points near the interface, are obtained. Simulations show that while the coherent scattered field

generally dominates, the incoherent scattered field is only essential around the Brewster angle for vv-polarisation. The phenomenon of depolarisation caused by the incoherent rough surface scattering is also studied. Generally, the incoherent scattered field becomes more significant as the observation point approaches the interface. Then, the solutions for the mean-field and incoherent scattered power generated by a small dipole of arbitrary orientation and position are derived by expanding the field of the dipole in terms of a continuous spectrum of plane waves and using superposition. Although it is found that the direct and coherent reflected (reflected+surface waves) fields are dominant in most cases, the incoherent scattering could be important, when the path along the line of sight is obscured.

6 Acknowledgment

This research was supported by National Science Foundation, ECE Program, under Award Number: 1101868.

7 References

- 1 Sommerfeld, A.: 'Partial differential equations in physics' (Academic Press, 1985)
- 2 Sarabandi, K., Chiu, T.: 'Electromagnetic scattering from slightly rough surfaces with inhomogeneous dielectric profiles', *IEEE Trans. Antennas Propag.*, 1997, **45**, (9), pp. 1419–1430
- 3 Tsang, L., Kong, J., Shin, R.T.: 'Theory of microwave remote sensing' (John Wiley and Sons, 1985)

- 4 Brown, R.G., Sharpe, R.A., Hughes, W.L., Post, R.E.: 'Lines, waves, and antennas: the transmission of electric energy' (The Ronald Press Company, 1992)
- 5 Balanis, C.A.: 'Advanced engineering electromagnetics' (John Wiley and Sons, 1989)
- 6 King, R.W.P., Sandler, S.S.: 'The electromagnetic field of a vertical electric dipole over the earth or sea', *IEEE Trans. Antennas Propag.*, 1994, **42**, (3), pp. 382–389
- 7 James, J.R., Hall, P.S.: 'Handbook of microstrip antennas' (Peter Peregrinus Ltd., 1989)
- 8 Hall, M.P.M., Barclay, L.W., Hewitt, M.T.: 'Propagation of radiowaves' (The Institution of Electrical Engineers, 1996)

8 Appendix

The expression for the N th order polarisation currents are given by

$$\begin{aligned}\tilde{J}_{Nh}(\mathbf{k}_\perp, z) &= \frac{ik_0^2(\epsilon - 1)}{k_z + k_{1z}} C_0^h(\mathbf{k}, z) [\tilde{V}_N \cdot \hat{h}(k_z)] \\ \tilde{J}_{Nt}(\mathbf{k}_\perp, z) &= \frac{ik_0 k_{1z}(\epsilon - 1)}{\epsilon k_z + k_{1z}} C_0^v(\mathbf{k}, z) [\tilde{V}_N \cdot \hat{v}(-k_z)] \\ \tilde{J}_{Nz}(\mathbf{k}_\perp, z) &= \frac{ik_0 k_\rho(\epsilon - 1)}{\epsilon k_z + k_{1z}} C_1^v(\mathbf{k}, z) [\tilde{V}_N \cdot \hat{v}(-k_z)]\end{aligned}$$

where (see equation at the bottom of the page)

where $*$ is the convolution operator, $F(\mathbf{k}_\perp)$ is the Fourier transform of $f(x', y')$ and $\overset{n}{\otimes}$ represents n -fold self-convolution ($\overset{n}{\otimes} F = \overbrace{F * F * \dots * F}^n$).

The second-order expressions for reflection coefficients used in (18) are given by (see (31) and (32))

The integrands in (27) are given by

$$\begin{aligned}P_Q^h(k_\rho) &= \int_0^{2\pi} d\phi [\mathbf{P} \cdot \hat{h}(k_z) \hat{h}(-k_z) \cdot \mathbf{Q}] e^{ik_\perp \cdot (\bar{\rho} - \bar{\rho}')} \\ &= \pi(P_x Q_x + P_y Q_y) J_0(k_\rho(|\bar{\rho} - \bar{\rho}'|)) \\ &\quad + \pi[(P_x Q_x - P_y Q_y) \cos(2\phi') + (P_x Q_y + P_y Q_x) \\ &\quad \times \sin(2\phi')] J_2(k_\rho(|\bar{\rho} - \bar{\rho}'|))\end{aligned}\tag{33}$$

$$\begin{aligned}P_Q^v(k_\rho) &= \int_0^{2\pi} d\phi [\mathbf{P} \cdot \hat{v}(k_z) \hat{v}(-k_z) \cdot \mathbf{Q}] e^{ik_\perp \cdot (\bar{\rho} - \bar{\rho}')} \\ &= \frac{\pi}{k_o^2} [2k_\rho^2 P_z Q_z - k_z^2 (P_x Q_x + P_y Q_y)] J_0(k_\rho(|\bar{\rho} - \bar{\rho}'|)) \\ &\quad + \frac{2\pi k_z k_\rho}{k_o^2} [(P_x Q_z - P_z Q_x) \cos \phi' \\ &\quad + (P_y Q_z - P_z Q_y) \sin \phi'] J_1(k_\rho(|\bar{\rho} - \bar{\rho}'|)) \\ &\quad + \pi \left(\frac{k_z}{k_o}\right)^2 [(P_x Q_x - P_y Q_y) \cos(2\phi') \\ &\quad + (P_x Q_y + P_y Q_x) \sin(2\phi')] J_2(k_\rho(|\bar{\rho} - \bar{\rho}'|))\end{aligned}\tag{34}$$

$$\phi' = \cos^{-1} \frac{(x - x')}{|\bar{\rho} - \bar{\rho}'|}$$

$$V_N = \sum_{n=0}^{N-1} \sum_{m=0}^{N-n-1} \frac{\binom{N-n-1}{m} (ik_z)^m}{(N-n)!} \cdot \left[\frac{\partial^{N-n-m-1}}{\partial(z')^{N-n-m-1}} \tilde{J}_n(\mathbf{k}_\perp, d) \right] * \overset{N-n}{\otimes} F(\mathbf{k}_\perp)$$

$$\begin{aligned}R_h^{(2)} &= k_z e^{-2ik_z d} \left\{ -2s^2 R_h k_{1z} C_0^h(\mathbf{k}, d) C_1^h(\mathbf{k}, d) + \frac{1}{2\pi^2} [C_0^h(\mathbf{k}, d)(k_z - k_{1z})]^2 \int d^2 \mathbf{k}'_\perp W(\mathbf{k}'_\perp - \mathbf{k}_\perp) \right. \\ &\quad \times \left. \left[\frac{C_0^h(\mathbf{k}', d) \cos^2(\phi'_k - \phi_k)}{k'_z + k'_{1z}} + \frac{k'_z k'_{1z} C_0^v(\mathbf{k}', d) \sin^2(\phi'_k - \phi_k)}{k_o^2 (\epsilon k'_z + k'_{1z})} \right] \right\}\end{aligned}\tag{31}$$

$$\begin{aligned}R_v^{(2)} &= k_z e^{-2ik_z d} \left\{ -s^2 \frac{(\epsilon - 1)(1 - R_v)(k_{1z}^2 - \epsilon k_\rho^2)}{\epsilon k_z + k_{1z}} C_0^v(\mathbf{k}, d) C_1^v(\mathbf{k}, d) + \frac{1}{2\pi^2} (\epsilon - 1)^2 \left\{ (1 - R_v)^2 C_0^v(\mathbf{k}, d) \int d^2 \mathbf{k}'_\perp W(\mathbf{k}'_\perp - \mathbf{k}_\perp) \right. \right. \\ &\quad \times \left. \left[\frac{k_o^2 C_0^h(\mathbf{k}', d) C_0^v(\mathbf{k}, d) \sin^2(\phi'_k - \phi_k)}{k'_z + k'_{1z}} + \frac{k'_z k'_{1z} C_0^v(\mathbf{k}', d) C_0^v(\mathbf{k}, d) \cos^2(\phi_k - \phi'_k)}{\epsilon k'_z + k'_{1z}} + \frac{k'_\rho k_\rho k'_{1z} C_0^v(\mathbf{k}', d) C_1^v(\mathbf{k}, d) \cos(\phi_k - \phi'_k)}{k_{1z} (\epsilon k'_z + k'_{1z})} \right] \right. \\ &\quad + (R_v - 1) \frac{2\epsilon k_\rho}{\epsilon k_z + k_{1z}} C_1^v(\mathbf{k}, d) \int d^2 \mathbf{k}'_\perp W(\mathbf{k}'_\perp - \mathbf{k}_\perp) \\ &\quad \times \left. \left. \left[\frac{k'_z k'_\rho C_1^v(\mathbf{k}', d) C_0^v(\mathbf{k}, d) \cos(\phi'_k - \phi_k)}{\epsilon k'_z + k'_{1z}} + \frac{k'_\rho k_\rho C_1^v(\mathbf{k}', d) C_1^v(\mathbf{k}, d) \cos^2(\phi_k - \phi'_k)}{k_{1z} (\epsilon k'_z + k'_{1z})} \right] \right\} \right\}\end{aligned}\tag{32}$$